

Sensitivity investigation of 100-MeV proton irradiation to SiGe HBT single event effect

Ya-Hui Feng(冯亚辉), Hong-Xia Guo(郭红霞), Yi-Wei Liu(刘益维), Xiao-Ping Ouyang(欧阳晓平), Jin-Xin Zhang(张晋新), Wu-Ying Ma(马武英), Feng-Qi Zhang(张凤祁), Ru-Xue Bai(白如雪), Xiao-Hua Ma(马晓华), and Yue Hao(郝跃)

Citation: Chin. Phys. B, 2024, 33 (**1**): 016104. DOI: 10.1088/1674-1056/acf303
Journal homepage: http://cpb.iphy.ac.cn; http://iopscience.iop.org/cpb

What follows is a list of articles you may be interested in

Analysis of displacement damage effects on the charge-coupled device induced by neutrons at Back-n in the China Spallation Neutron Source

Yuan-Yuan Xue(薛院院), Zu-Jun Wang(王祖军), Wei Chen(陈伟), Xiao-Qiang Guo(郭晓强), Zhi-Bin Yao(姚志斌), Bao-Ping He(何宝平), Xu Nie(聂栩), Shankun Lai(赖善坤), Gang Huang(黄港), Jiang-Kun Sheng(盛江坤), Wu-Ying Ma(马武英), and Shi-Long Gou(缑石龙)

Chin. Phys. B, 2023, 32 (**7**): 076101. DOI: 10.1088/1674-1056/acac07

Sensitivity study of the SiGe heterojunction bipolar transistor single event effect based on pulsed laser and technology computer-aided design simulation

Ya-Hui Feng(冯亚辉), Hong-Xia Guo(郭红霞), Xiao-Yu Pan(潘霄宇), Jin-Xin Zhang(张晋新),Xiang-Li Zhong(钟向丽), Hong Zhang(张鸿), An-An Ju(琚安安),Ye Liu(刘晔), and Xiao-Ping Ouyang(欧阳晓平)

Chin. Phys. B, 2023, 32 (**6**): 066105. DOI: 10.1088/1674-1056/ac8f3b

Impact of proton-induced alteration of carrier lifetime on single-event transient in SiGe heterojunction bipolar transistor

Jia-Nan Wei(魏佳男), Chao-Hui He(贺朝会), Pei Li(李培), Yong-Hong Li(李永宏), Hong-Xia Guo(郭红霞)

Chin. Phys. B, 2019, 28 (**7**): 076106. DOI: 10.1088/1674-1056/28/7/076106

Mechanism of floating body effect mitigation via cutting off source injection in a fully-depleted silicon-on-insulator technology

Pengcheng Huang(黄鹏程), Shuming Chen(陈书明), Jianjun Chen(陈建军)

Chin. Phys. B, 2016, 25 (**3**): 036103. DOI: 10.1088/1674-1056/25/3/036103

Mechanism of single-event transient pulse quenching between dummy gate isolated logic nodes

Chen Jian-Jun (陈建军), Chi Ya-Qing (池雅庆), Liang Bin (梁斌)

Chin. Phys. B, 2015, 24 (**1**): 016102. DOI: 10.1088/1674-1056/24/1/016102

Sensitivity investigation of 100-MeV proton irradiation to SiGe HBT single event effect

Ya-Hui Feng(冯亚辉)[1], Hong-Xia Guo(郭红霞)[2,4,†], Yi-Wei Liu(刘益维)[2], Xiao-Ping Ouyang(欧阳晓平)[1,4], Jin-Xin Zhang(张晋新)[3], Wu-Ying Ma(马武英)[4], Feng-Qi Zhang(张凤祁)[4], Ru-Xue Bai(白如雪)[2], Xiao-Hua Ma(马晓华)[1], and Yue Hao(郝跃)[1]

[1] *State Key Laboratory of Wide Bandgap Semiconductor Devices, School of Microelectronics, Xidian University, Xi'an* 710071, *China*
[2] *School of Materials Science and Engineering, Xiangtan University, Xiangtan* 411105, *China*
[3] *School of Space Science and Technology, Xidian University, Xi'an* 710071, *China*
[4] *State Key Laboratory of Experimental Simulation and Effects of Strong Pulse Radiation, Northwest Institute of Nuclear Technology, Xi'an* 710024, *China*

(Received 14 July 2023; revised manuscript received 15 August 2023; accepted manuscript online 23 August 2023)

The single event effect (SEE) sensitivity of silicon–germanium heterojunction bipolar transistor (SiGe HBT) irradiated by 100-MeV proton is investigated. The simulation results indicate that the most sensitive position of the SiGe HBT device is the emitter center, where the protons pass through the larger collector-substrate (CS) junction. Furthermore, in this work the experimental studies are also carried out by using 100-MeV proton. In order to consider the influence of temperature on SEE, both simulation and experiment are conducted at a temperature of 93 K. At a cryogenic temperature, the carrier mobility increases, which leads to higher transient current peaks, but the duration of the current decreases significantly. Notably, at the same proton flux, there is only one single event transient (SET) that occurs at 93 K. Thus, the radiation hard ability of the device increases at cryogenic temperatures. The simulation results are found to be qualitatively consistent with the experimental results of 100-MeV protons. To further evaluate the tolerance of the device, the influence of proton on SiGe HBT after gamma-ray (^{60}Coγ) irradiation is investigated. As a result, as the cumulative dose increases, the introduction of traps results in a significant reduction in both the peak value and duration of the transient currents.

Keywords: silicon–germanium heterojunction bipolar transistor (SiGe HBT), 100-MeV proton, technology computer-aided design (TCAD), single event effect (SEE)

PACS: 61.72.uf, 61.80.Ed, 61.80.–x, 61.80.Jh **DOI:** 10.1088/1674-1056/acf303

1. Introduction

The silicon–germanium heterojunction bipolar transistor (SiGe HBT) represents a key device for aerospace applications. It has become a very promising candidate for developing electronic systems used for extreme environments.

This is due to its intrinsic ability to withstand high levels of total ionizing dose and displacement damage effects.[1–3] Furthermore, the SiGe HBT device exhibits remarkable characteristics such as low noise, high frequency, and high power gain performance.[4] Previous research has demonstrated that the SiGe HBT is the sole electronic device of functioning normally in a range of electronic devices at cryogenic temperatures.[5,6] Nevertheless, the SiGe HBT devices are highly sensitive to single-event effects (SEEs), which is a noteworthy concern.[7] The concept of extreme environments includes two distinct aspects, namely space radiation and environments characterized by extreme temperatures. For instance, the surface of the Moon is subject to extreme temperature conditions, with worst cases reaching as low as −230 °C in the shadowed polar craters.[4] Moreover, temperatures on the lunar surface can fluctuate dramatically, ranging from −180 °C during the lunar night to +120 °C during the lunar day. Europa, one of Jupiter's moons, experiences nighttime surface temperatures spanning from −141 °C to +213 °C.[8] The radiation environment that is of particular interest for satellites and spacecrafts in orbit is comprised of charged particles that become trapped by the Earth's magnetic field, as well as galactic and solar cosmic rays.[8]

In general, the equipment using gamma-ray (^{60}Coγ), protons, and neutrons is usually used to study the reliability of semiconductor devices. Numerous researchers have extensively investigated the effects of these forms of radiations on silicon bipolar junction transistors (BJTs).[9] Notably, existing literature shows that there are relatively few studies on the sensitivity of 100-MeV proton irradiation to SiGe HBT SEEs, especially in low temperature environment. Within the context of space irradiation environments, protons account for over 90 percent of the total irradiation particles.[10] The degradation of device characteristics induced by energetic protons can occur via both non-ionizing energy loss process and ionizing energy loss process. Furthermore, it is worth noting that protons with energy as high as several hundreds of MeVs are the main reason for the failure of electronic device in low Earth orbit.[11]

Therefore, the focus of this work is to study the sensitivity of 100-MeV proton irradiation to SiGe HBT SEE. Furthermore, in order to gain a more in-depth understanding of the

[†]Corresponding author. E-mail: guohxnint@126.com

© 2024 Chinese Physical Society and IOP Publishing Ltd

influence of transport mechanism on SEE, a two-dimensional (2D) structure of the SiGe HBT device is established by using TCAD simulation tool. The influence of temperature on the SEE of SiGe HBT cannot be ignored. Hence, in order to investigate its influence, both simulation and proton experiments are conducted at a temperature of 93 K.

2. Sample induction and experiment methods

2.1. Sample introduction

The SiGe HBT investigated in this work is available from Tsinghua University. The fabricated SiGe HBT is a vertical type composed of a 90-nm-wide base, a 2.12-μm-wide collector, and a 253-nm-wide emitter, respectively.

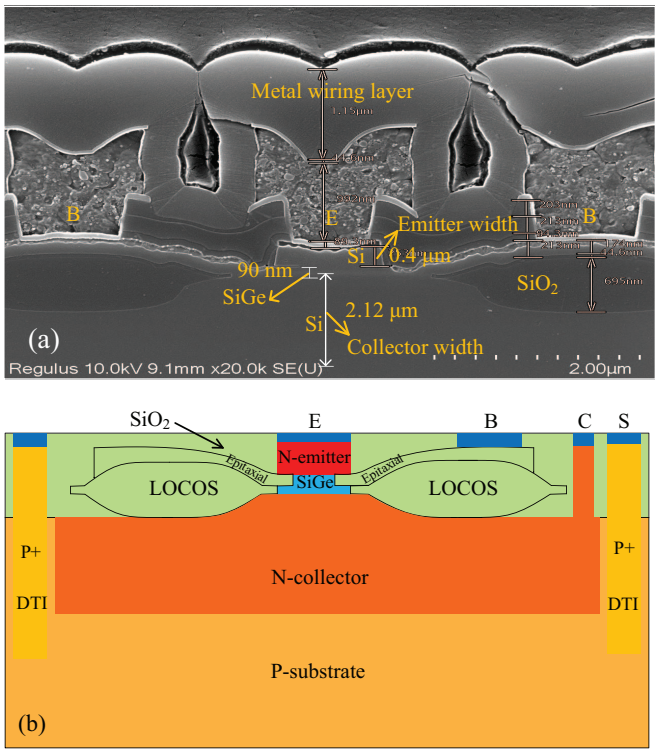


Fig. 1. (a) SEM image of fabricated device and (b) schematic cross-section of vertical SiGe HBT.

The shallow trench isolation (STI) is 695-nm thick, and aluminum layer is 695-nm thick. The distance between beaks is 1.96 μm. The device lithographic node, or emitter geometry, is 0.4 μm×20 μm in size. The scanning electron microscopy (SEM) image of a fabricated SiGe HBT device, is shown in Fig. 1(a). The schematic cross-section of the vertical SiGe HBT, which only displays the SiGe HBT structure without the metal wiring layer above it, is shown in Fig. 1(b). The doping concentration of the N-emitter is 6.34×10^{19} cm^{-3}, showing a Gaussian distribution. In the intrinsic P-base, germanium is introduced to form SiGe alloy and lower the barrier height. The doping concentration of the region is 1.6×10^{19} cm^{-3}, showing a Gaussian distribution. The intrinsic N-collector of SiGe HBT is doped with a concentration of 1.5×10^{18} cm^{-3}, showing a Gaussian distribution. The direct current (DC) gain of the device (h_{EF}) is in a range of 50–100 at $V_{CE} = 2$ V and $I_C = 25$ mA. The breakdown voltage of collector–base (BV_{CBO}) is 9 V at $I_C = 2.5$ μA and $I_E = 0$, the breakdown voltage of collector–emitter (BV_{CEO}) is 4.5 V at $I_C = 1$ mA and $I_B = 0$, and the breakdown voltage of emitter–base (BV_{EBO}) is 1 V at $I_E = 2.5$ μA and $I_C = 0$.

2.2. Setting of experimental conditions

In order to accurately capture the single event transients (SETs), the model of the MSO464-BW-1500 oscilloscope with a bandwidth of 1 GHz–15 GHz and sample rate of 1–50 gigasamples·s^{-1} and the Bias Tees (wideband ZX85-12G+ from 0.2 MHz to 12 GHz) powered by Mini-Circuits are used. We also use low-loss SMA coaxial cables to connect the test path and a DC power apply bias on each electrode of the device under test (DUT). Owing to the fact that the collector of the DUT is usually used as the output terminal, the SET waveforms of the collector terminal are studied. Meanwhile, in order to create a low-temperature radiation environment, a temperature control system of the LNT-500 is customized. The system is capable of achieving a pressure of 0.1 Pa and has a maximum theoretical controllable temperature range from 80 K to 500 K. Room temperature of 300 K and the project assessment temperature of 93 K (−180 °C) are selected for the testing process. In this work, the SEE of SiGe HBT is studied under the condition of both cut-off and forward amplification bias. In order to accurately investigate the SEE of SiGe HBT, secondary particles generated by the irradiation of 100-MeV protons are taken into account by using Geant4 (GEometry AND Tracking) software as shown in Table 1.

Table 1. Secondary particles are produced by 100-MeV proton nuclear reactions.

Secondary particle	Maximum energy	LET (MeV·cm^2·mg^{-1})	Average range (μm)	Share (%)
C	7.0	5.0	7.2	
N	3.3	6.2	3.1	0.3
O	14.2	7.1	9.3	
F	6.7	8.6	5.0	0.6
Ne	9.8	9.5	6.2	0.7
Na	15.4	10.3	8.2	3.1
Mg	13.0	11.5	6.8	9.4
Al	9.2	11.5	5.4	15.4
Si	7.1	12.4	3.9	69.5
P	2.6	10.4	2.0	1.0

3. Discussion and analysis

3.1. Mechanism analysis ofSETs

Protons incident on SiGe HBT generate nuclear reactions, producing various secondary particles. The properties of these secondary particles are obtained by using the Geant4 software, and they are summarized in Table 1. In order to carry out

an SEE simulation , these parameters are introduced into the sentaurus TCAD simulation tool. In order to accurately simulate the SEEs, the Philips unified mobility model, velocity saturation, bandgap narrowing, incomplete ionization, impact ionization, Fermi statistics, Read, and temperature-dependent Auger recombination are incorporated into the TCAD simulation tools.[12,13]

According to Fig. 2, given that the proportion of Si particles is the largest in the generated secondary particles.

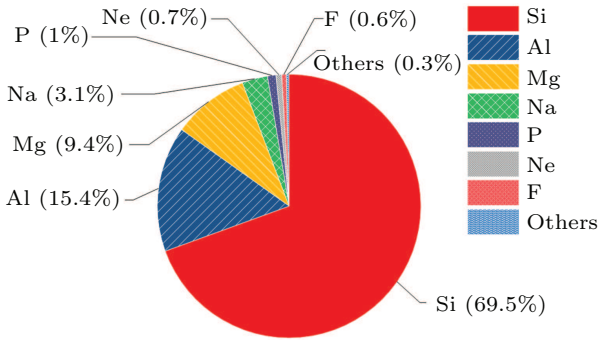


Fig. 2. Percentages of various secondary particles.

For one thing, the electrical characteristics of the SiGe HBT are calibrated by adjusting a series of model parameters, which are doping concentration, the structure of device, and carrier mobility. The heavy ion incidence model is introduced within the physics module. In the 2D simulation, the generation rate of electron–hole pairs can be obtained from the following equation:[14]

$$\text{Rate}(l,\omega,t) = G_{\text{LET}}(l)\,R(\omega,l)\,T(t), \tag{1}$$

where $R(\omega,l)$ and $T(t)$ are the spatial distribution and temporal distribution of the generation rate, respectively, ω is the radius defined as the perpendicular distance from the track, l is the length of the track, $G_{\text{LET}}(l)$ is the LET (linear energy transfer) generation density. The simulation results are qualitative rather than quantitative owing to the fact that the distribution of the carriers is not cylindrical along the ion incident track.[15]

At the different incident positions and voltage bias states, the potential collapse and electric field effects produced by secondary particle incidence are obtained as shown in Fig. 3. From Fig. 3, it can be concluded that the potential collapse generated at the same incident position at bias voltage $V_{\text{CE}} = 3$ V and $V_{\text{BE}} = 0$ V is more pronounced than at $V_{\text{CE}} = 5$ V and $V_{\text{BE}} = 0$ V. From the contours it can be concluded that with the increase of bias voltage, the electrical potential increases at the same distance, *i.e.*, the electric field turns larger and the carriers acquire a larger drift velocity as they are collected, resulting in an increase in the peak value of the SET current. The comparison among Figs. 3(1a), 3(2a), and 3(3a) or 3(1b), 3(2b), and 3(3b) shows that the most pronounced potential collapse is produced by incidence from the centre of the emitter under the same bias conditions. SETs generated by the incidence of various secondary particles are obtained[16,17] as shown in Figs. 4. The research results indicate that as the collector bias decreases, the peak value of the transient current decreases as shown in Table 2. However, the duration of the transient current increases at the same ion incident position. This phenomenon can be attributed to the drift velocity of carrier and the collection amount of the charge reduction at a unit time, owing to collector bias voltage decreasing.[18,19] Consequently, it takes a long time to correct the electron–hole pairs generated by ionization along the incident track.

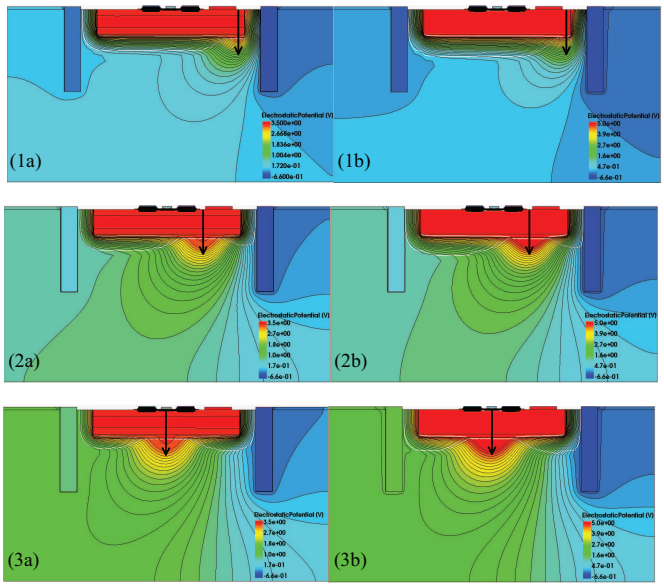


Fig. 3. Potential collapse and electric field effects produced by secondary particle incidence from [(1a), (1b)] collector boundary, [(2a), (2b)] gap between base and collector, and [(3a), (3b)] emitter center, respectively.

Moreover, it can be concluded that when the incidence is from the emitter center, the device is particularly susceptible to SEE. This phenomenon can be attributed to the fact that when an incident occurs from the emitter center, the incident track passes not only through the larger collector/substrate (CS) junction, which is the most sensitive position of the device,[20,21] but also through all electrode areas of the device. As a result, a significant potential collapse occurs, causing the electron–hole pairs to be quickly collected by drift under the action of the electric field to form a large transient current peak as shown in Figs. 4(3a) and 4(3b).

In Table 1, position 1, position 2, and position 3 are defined as the collector boundary, the gap between the base and collector, and the emitter center, respectively; Δ_1 is the difference between the peak of the collector transient current at $V_{\text{CE}} = 5$ V and $V_{\text{CE}} = 3$ V; Δ_2 is the difference between the duration of the collector transient current at $V_{\text{CE}} = 5$ V, $V_{\text{BE}} = 0$ V and $V_{\text{CE}} = 3$ V, $V_{\text{BE}} = 0$ V as shown in Table 3.

Table 2. Variations of SET produced by secondary particle incidence under different bias conditions.

Incident position	Bias condition (V)	Peak value (P_3)	Bias condition (V)	Peak value (P_5)	$\Delta_1 = P_5 - P_3$
Position 1	$V_{CE} = 3$ $V_{BE} = 0$	0.6	$V_{CE} = 5$ $V_{BE} = 0$	0.74	0.14
Position 2	$V_{CE} = 3$ $V_{BE} = 0$	0.17	$V_{CE} = 5$ $V_{BE} = 0$	0.24	0.07
Position 3	$V_{CE} = 3$ $V_{BE} = 0$	0.9	$V_{CE} = 5$ $V_{BE} = 0$	1.23	0.33

Table 3. Durations of SETs produced by secondary particle incidence under different bias conditions.

Temperature	Bias condition (V)	Duration of current T_3 (ns)	Bias condition (V)	Duration of current T_5 (ns)	$\Delta_2 = T_3 - T_5$ (ns)
Position 1	$V_{CE} = 3$ $V_{BE} = 0$	0.95	$V_{CE} = 5$ $V_{BE} = 0$	0.65	0.3
Position 2	$V_{CE} = 3$ $V_{BE} = 0$	2.34	$V_{CE} = 5$ $V_{BE} = 0$	2.1	0.24
Position 3	$V_{CE} = 3$ $V_{BE} = 0$	0.26	$V_{CE} = 5$ $V_{BE} = 0$	0.19	0.07

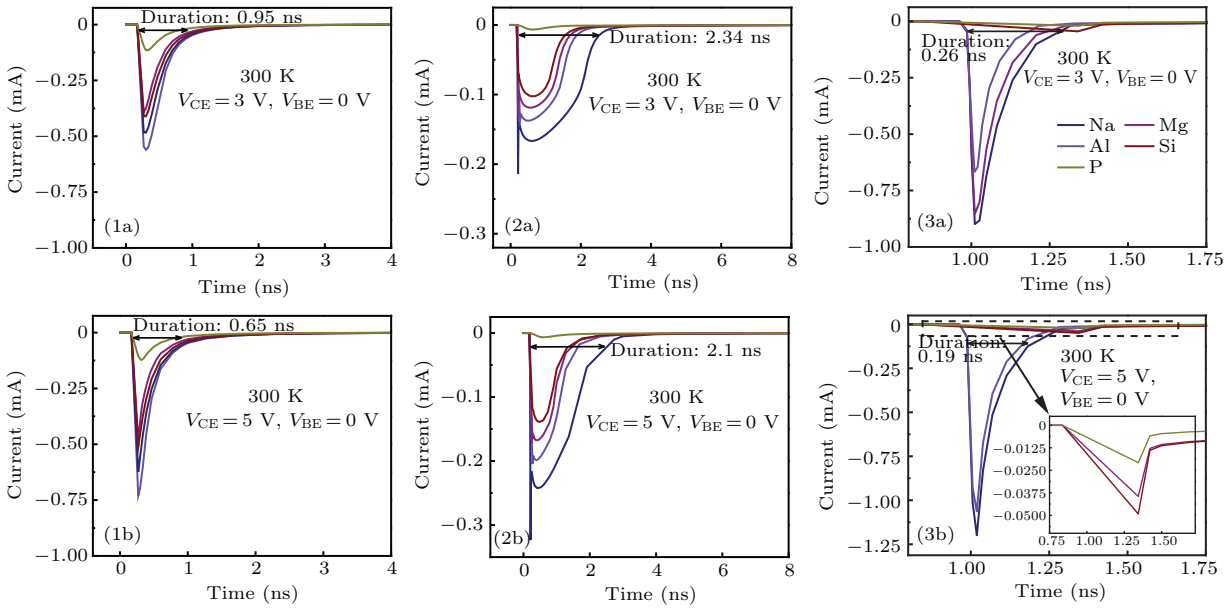


Fig. 4. The TCAD calculated the collector transient currents caused by secondary particles incident from [(1a), (1b)] collector boundary and [(2a), (2b)] gap between base and collector, and [(3a), (3b)] emitter center, respectively.

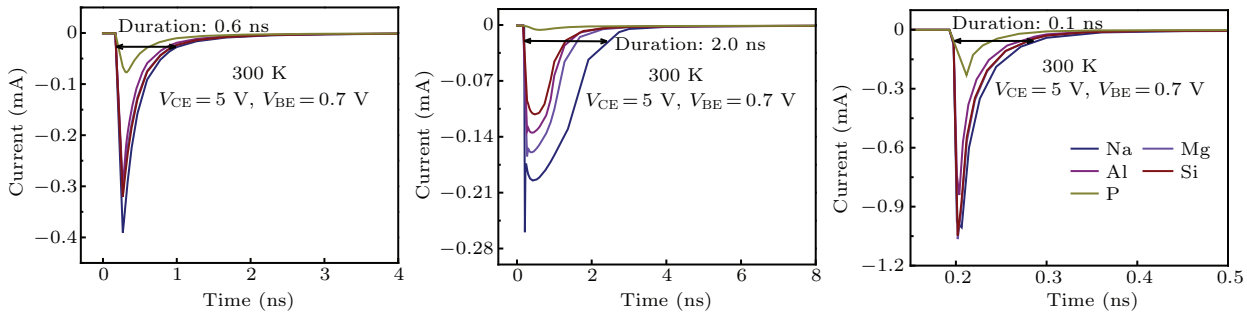


Fig. 5. Under forward amplification bias, collector transient currents caused by secondary particles incident from (a) collector boundary, (b) gap between base and collector, and (c) emitter center, respectively.

In order to gain a more comprehensive understanding of the device's radiation tolerance, the sensitivity of the SEE is further investigated under the forward amplification bias conditions ($V_C = 5$ V, $V_B = 0.7$ V) as shown in Fig. 5. The research results reveal that when the particle hits the emitter center, the SET peak observed under the forward amplification bias conditions is significantly lower than that observed under the cut-off bias conditions ($V_C = 5$ V, $V_B = 0$ V) as shown in Table 4. The charge collection mechanism for this phenomenon is that the electrons flow from the emitter of the SiGe HBT device to

the collector, and across the base, where they are collected in the respective regions. Conversely, the holes move in the opposite direction towards the region of lower potential, where they are collected by the emitter. The quantity of charge collected in this manner continues to increase over time. The results indicate that the sensitivity of SiGe HBT to SEE decreases under the forward amplification bias conditions.

As shown in Table 4, Δ_3 is the difference between the peak of the collector transient current at $V_{CE} = 5$ V and $V_{BE} = 0$ V and the peak of the collector transient curren at $V_{CE} = 5$ V and $V_{BE} = 0.7$ V. Δ_4 is the difference between the duration of the collector transient current at $V_{CE} = 5$ V and $V_{BE} = 0$ V and the duration of the collector transient current at $V_{CE} = 5$ V, $V_{BE} = 0.7$ V, as shown in Table 5.

Table 4. Variations of SETs produced by secondary particle incidence under different bias conditions.

Incident position	Bias condition (V)	Peak value	Bias condition (V)	Peak value	$\Delta_3 = P_5 - P_3$
Position 1	$V_{CE} = 5$ $V_{BE} = 0.7$	0.38	$V_{CE} = 5$ $V_{BE} = 0$	0.74	0.36
Position 2	$V_{CE} = 5$ $V_{BE} = 0.7$	0.20	$V_{CE} = 5$ $V_{BE} = 0$	0.24	0.04
Position 3	$V_{CE} = 5$ $V_{BE} = 0.7$	1.06	$V_{CE} = 5$ $V_{BE} = 0$	1.23	0.17

Table 5. Duration of SETs produced by secondary particle incidence under different bias conditions.

Temperature	Bias condition (V)	Duration of current T_3 (ns)	Bias condition (V)	Duration of current T_5 (ns)	$\Delta_4 = T_5 - T_3$ (ns)
Position 1	$V_{CE} = 5$ $V_{BE} = 0.7$	0.6	$V_{CE} = 5$ $V_{BE} = 0$	0.65	0.05
Position 2	$V_{CE} = 5$ $V_{BE} = 0.7$	2.0	$V_{CE} = 5$ $V_{BE} = 0$	2.1	0.1
Position 3	$V_{CE} = 5$ $V_{BE} = 0.7$	0.1	$V_{CE} = 5$ $V_{BE} = 0$	0.19	0.09

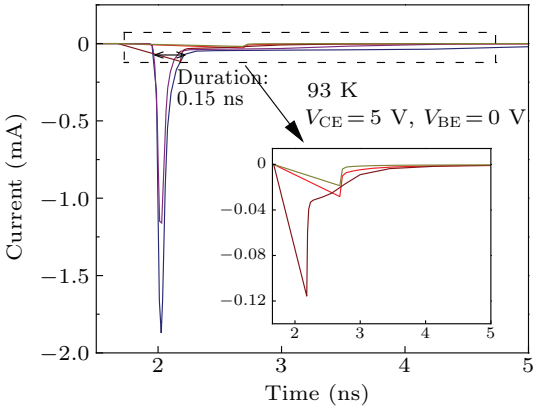


Fig. 6. Time-dependent collector currents caused by secondary particles incident from emitter center at a cryogenic temperature (93 K).

The extreme environment includes two aspects: space radiation and extreme temperature environment. In order to explore this further, the simulation of the SEE of the SiGe HBT device is carried out at a cryogenic temperature,[5] as shown in Fig. 6.

In the simulation of cryogenic temperature, bandgap narrowing model, carrier mobility model, tunneling model, and so forth are introduced into physics module. The simulation results indicate that the transient current peak value of collector increases from 1.23 mA at 300 K to the 1.9 mA at 93 K as depicted in Figs. 4(3b) and 6. Some peak values drop, only reaching a value of about 0.12 mA, which is considered negligible in the case of the 100-MeV proton experiment, for example, the partial enlargement is detailed in Fig. 6. However, it is noteworthy that the duration of the transient current is significantly reduced. The primary reason for the observed phenomenon is that the influence of lattice scattering on carrier mobility decreases at cryogenic temperatures. Concomitantly, there is an increase in mobility, which leads to an increased drift velocity.[22–24] As a result of this increased mobility, carriers generated via ionization can be quickly collected at per unit of time through drift under the action of an electric field.[12,25] Moreover, a portion of the collector current is explained by using a direct tunneling mechanism from the emitter to the collector at cryogenic temperatures.[26] Consequently, the transient current with a large peak value is formed as expected by Eq. (2). Previous research has demonstrated that the LET threshold of SiGe HBT for triggering an SEE is positively correlated with temperature reduction.[27] Based on the above, it can be concluded that SiGe HBT exhibits decreased susceptibility to SEE at cryogenic temperatures. The current caused by secondary particles incident from the emitter center at a cryogenic temperature is expressed as

$$i(t) = -eN\mu' E_0 \left(\mathrm{e}^{-\mu' E' t} - \mathrm{e}^{-\beta t} \right), \tag{2}$$

where N is the total charge injected, E_0 is the maximum electric field, $1/\beta$ is the time constant for establishing the initial ion track, and $\mu' = 1/2\left(\mu_n + \mu_p\right) F(E)$ is an average mobility, μ_n and μ_p represent the mobility of electrons and holes,

respectively. $F(E)$ is a correction factor.

3.2. SETs of SiGe HBT based on 100-MeV proton irradiation experiments

Experiments are carried out at Xi'an 200-MeV Proton Application Facility (XiPAF). The 100-MeV proton with a fixed fluence rate of 1×10^{8} p·cm^{-2}·s^{-1} is selected to conduct research under different conditions. The proton beam spot size is 1 cm×1 cm. The SEEs of the SiGe HBT device are investigated under the cut-off amplification bias condition and the forward amplification bias condition, respectively.

The interaction of protons with the silicon lattice results in both inelastic collisions and elastic collisions, creating secondary particles that possess sufficient range and energy to ionize the material along the incident track.[23,28] This process generates electron–hole pairs that can subsequently be collected through drift and diffusion to form an SET. In order to gain a better understanding of the underlying transport mechanisms, the radiation results at temperatures ranging from 93 K to 433 K are comparatively analyzed as shown in Fig. 7.

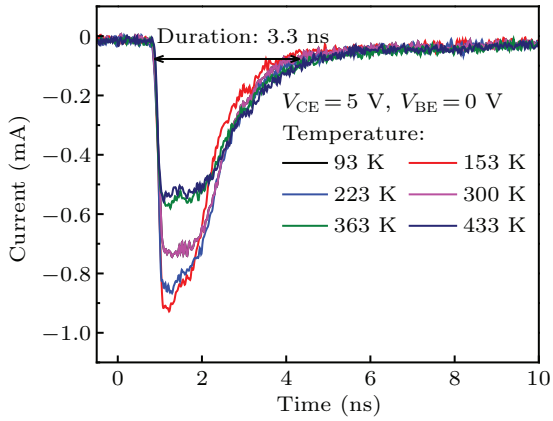


Fig. 7. Time dependent effects of temperature on SETs of SiGe HBTs.

The results show that the peak value of the SET current increases and the current duration decreases as the temperature decreases. The reason for this phenomenon is that the effect of lattice scattering on the carrier mobility decreases as the temperature decreases, which makes the carriers collected in a shorter time to obtain a larger transient current. When the temperature reaches 153 K, the transient current does not change significantly as the temperature continues to decrease, owing to the effect of incomplete ionization. At extreme low temperatures, SiGe HBT overcomes the carrier freeze-out effect and possesses superior low temperature characteristics in comparison with the counterparts in other devices. Therefore, its susceptibility to SEE at low temperatures is investigated more in this work.

In order to gain further understanding of the underlying transport mechanisms, the radiation results at the temperature of 93 K and 300 K are comparatively analyzed. For one thing, when the 100-MeV proton irradiation is used experimentally to investigate the sensitivity of SiGe HBT SEE, the device is subject to cut-off bias states at both 93 K and 300 K, respectively.

The results indicate that the peak values of the SET generated by the incident 100-MeV protons become greater as the temperature decreases. That is, 0.75 mA at the temperature of 93 K is comparable to 0.65 mA at the temperature of 300 K as shown in Fig. 8. Comparative analysis reveals that in contrast to the case at 300 K, there is only an SET is generated at 93 K. Moreover, the duration of the transient current is also shorter under the same conditions. The main reason is that the influence of scattering on carrier mobility decreases at cryogenic temperatures, thereby leading the electron–hole pairs produced by ionization to be able to be quickly collected via drift under the action of the electric field.[24,25,29] It is also concluded that a higher field and mobility result in higher peak current, faster rise time, and faster fall time, owing to the faster carrier drift velocity from Eq. (2). Therefore, the duration of the transient current is found to be shorter at 93 K.

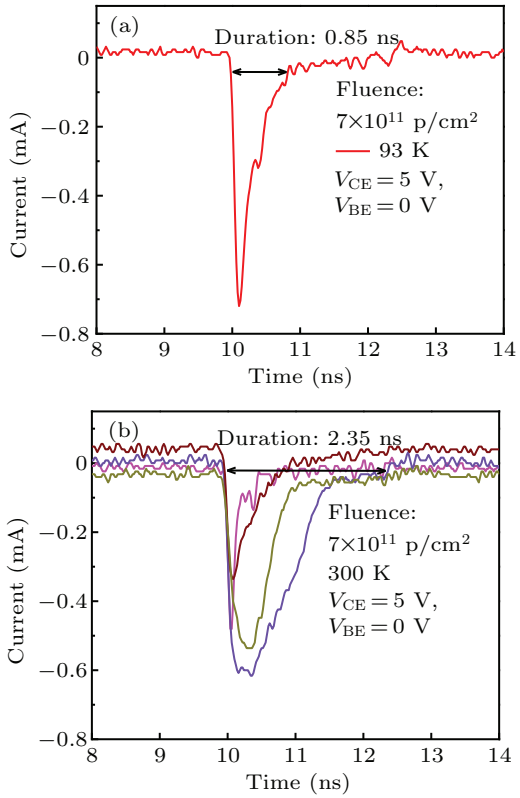


Fig. 8. SETs of collector generated by proton incident at 93 K (a) and 300 K (b).

In addition, when the proton fluence reaches the value 7×10^{11} p/cm^2, the unique SET waveform is triggered by the incidence of various secondary particles at a cryogenic temperature of 93 K as shown in Fig. 8(a). However, multiple SET waveforms are detected at 300 K when the fluence is accumulated to 5.7×10^{11} p/cm^2 as shown in Fig. 8(b). In order to be consistent with the accumulated fluence at 93 K, the proton

fluence is also accumulated to 7×10^{11} p/cm^2, but the SETs do not change with the increase of proton fluence subsequently. The peak value of transient current is primarily by the carrier mobility (which increases with cooling due to the reduction in phonon scattering).[30] Thus, the current peak is higher than that at 300 K. According to the number of SETs and the duration of the SETs produced by incident 100-MeV protons, it is concluded that the SEE is more likely to occur at 300 K than at 93 K as shown in Figs. 8(a) and 8(b). In other words, the radiation hard ability of the device increases at cryogenic temperatures.

In order to further understand the damage and transport mechanisms of SiGe HBT devices, the experiment on 100-MeV proton irradiation is performed at room temperature (300 K). The research results for different bias states ($V_{CE}=5$ V, $V_{BE}=0$ V; and $V_{CE}=5$ V, $V_{BE}=0.7$ V) are presented and discussed below.

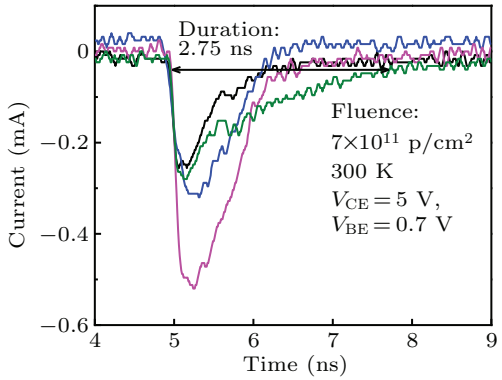


Fig. 9. SETs of collector generated by incident protons under forward amplification bias.

Multiple SET waveforms are detected by using a proton fluence of 7×10^{11} p/cm^2. Subsequently, in the process of increasing the fluence to 7.18×10^{11} p/cm^2 continuously, the SETs remain unchanged. In order to be consistent with the experimental proton fluence of Fig. 8, the data of SETs at the fluence of 7×10^{11} p/cm^2 are taken as the experimental results as shown in Fig. 9.

Figures 8(b) and 9 depict a comparative analysis of SETs generated under the cut-off bias and the forward amplification bias as elaborated in the following discussion. Results reveal that the peak values of the transient currents are lower than the counterparts in Fig. 8(b). Conversely, the duration of the transient current is generally observed to increase, as illustrated in Fig. 9. The main reason is that under the condition of forward amplification bias, the positive bias forms at the EB junction and the reverse bias forms at BC junction, which is is beneficial to the electrons from emitter to be collected by collector and base respectively. However, the quantity of the charge collection decreases in a unit time, resulting in the reduction of the peak value of the collector transient current. Therefore, the duration of the transient current increases generally. According to the charge formulation (Eq. (3)), it is well-known that a larger transient current is generated through the collection of higher quantity of charge within a unit of time. Quantity of charge (Q) is related to current (I), and time (t) as follows:

$$Q = I \cdot t. \tag{3}$$

With the cut-off bias state of $V_{CE}=5$ V, $V_{BE}=0$ V as a reference at 300 K, as shown in Table 6, it is concluded that the peak values of SETs obtained by both experiment and simulation at 93 K increase compared with those at 300 K under the same bias conditions. For the same temperatures, both experimental and simulated results show that the peak value of SET obtained under forward amplification bias is smaller than that obtained under cut-off bias.

It is worthwhile to note that the simulated trend of the peak variation of SETs is qualitatively consistent with measured one as shown in the above figures and Table 6.

Table 6. Peak values of SET under different conditions.

Temperature (K)	Bias condition	Experimental results (mA)	Simulation results (mA)
300	$V_{CE}=5$ V $V_{BE}=0.7$ V	0.55	1.06
	$V_{CE}=5$ V $V_{BE}=0$ V	0.65	1.23
93	$V_{CE}=5$ V $V_{BE}=0$	0.75	1.9

3.3. Influence of ^{60}Co γ irradiation on susceptibility to 100-MeV proton SETs

Likewise, the SiGe HBT devices are exposed to a complex space environment for operating, which will encounter a variety of factors, such as a variety of radiation particles, and extreme temperature environment. Among all the space radiation particles, protons account for the most significant proportion. Although the dose rate of ^{60}Co γ radiation is low in the space radiation environment, prolonged exposure to the space radiation environment may result in the total ionizing doses effect that can potentially affect their performance. In order to make the device run as close as possible to the actual radiation environment, it is important to study the effects of ^{60}Co γ and proton irradiation on the device.[31,32] Thus, in order to simulate real-life conditions that devices may encounter when operating in space radiation environments, investigations are performed by using both the Northwest Institute of Nuclear Technology ^{60}Co γ radiation source and XiPAF.

In this study, two sets of devices are irradiated by ^{60}Co γ source at a dose rate of 50 rad(Si)/s, until reaching cumulative doses of 500 krad(Si) and 1 Mrad(Si), respectively. During

exposure, all terminals of all devices are grounded.[33] Subsequently, the devices are subjected to irradiation by using 100-MeV proton to enable the further research and analysis after their exposure to ^{60}Co γ radiation.

Based on the analysis of Figs. 10(a)–10(c), it can be inferred that when the devices are exposed to ^{60}Co γ radiation the duration of the collector transient current is observed, in general, to be shorter at the cumulative dose of 1 Mrad(Si) than at the cumulative dose of 500 krad(Si) and the fresh. However, significant variations in the peak of the collector transient current resulting from the incident protons are observed at the cumulative doses of 1 Mrad(Si), 500 krad(Si), and the fresh, respectively. It is concluded that the peak value of collector transient current induced by the incident 100-MeV protons is the largest in the devices thatare not irradiated by ^{60}Co γ.

As the cumulative dose of ^{60}Co γ radiation increases, a large number of electron–hole pairs are generated within the oxide layer of the device. Owing to the remarkably large mobility of electrons, they are quickly moved away from the oxide layer, while the trapping of holes within the oxide layer leads to the creation of both interfacial charges and oxide-trap charges, respectively.[34] Moreover, during ^{60}Co γ radiation, an electric field pointing from collector to base is formed at the B/C junction by the cut-off bias so that the ionized holes transit towards the base side in the LOCOS (Location Oxidation of Silicon) and generate stable positive oxide-trap charges near the base, forming space electric field. While the SEE of the SiGe HBT device is studied by using 100-MeV proton, this space electric field whose direction is from base to collector diminishes the applied voltage of $V_{\rm C} = 5$ V.[31] Thereby, this is also the main reason why the peak value of the collector transient current decreases with the cumulation dose increasing.

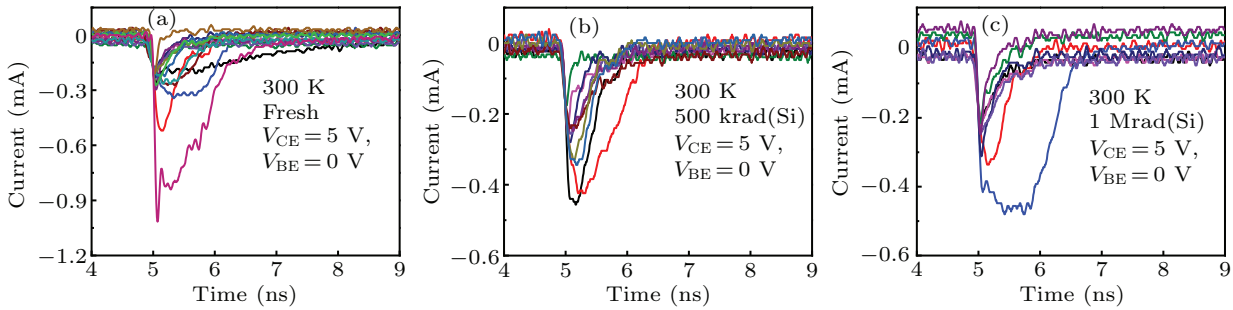


Fig. 10. Effects of proton irradiation on SiGe HBTSEE at a cumulative dose of (a) fresh, (b) 500 krad(Si), and (c) 1 Mrad(Si) of ^{60}Co γ, respectively.

4. Conclusions

The SEE of the SiGe HBT device is studied by using TCAD simulation tool and 100-MeV protons under different conditions. The simulation results indicate that the emitter center of the SiGe HBT device is the most susceptible to SETs due to crossing the larger CS junction. Meanwhile, the effects of temperature and bias conditions on the sensitivity of the SEE are also investigated. The research results show that the peak value of transient current increases with the increase of collector bias voltage. The sensitivity of the SEE decreases under the forward amplification bias conditions in comparison with under the cut-off bias condition, while the radiation tolerance capability of the SiGe HBT device is improved at a cryogenic temperature. From the qualitative point of view, the measured results are in good agreement with the simulated results. Finally, the effect of ^{60}Co γ radiation and proton radiation on the device are investigated. After SiGe HBT is irradiated by using ^{60}Co γ, with the increase of cumulative dose, the peak values of collector transient current caused by incident 100-MeV protons are obviously reduced, and the duration is also generally reduced due to the introduction of traps into the oxide layer of the SiGe HBT. The research results can provide important theoretical references for radiation-resistant reinforcement of devices in the aerospace environment.

Acknowledgement

Project supported by the National Natural Science Foundation of China (Grant Nos. 61574171, 61704127, 11875229, 51872251, and 12027813).

References

[1] Bellini M, Jun B, Sutton A K, Appaswamy A C, Cheng P, Cressler J D, Marshall P W, Schrimpf R D, Fleetwood D M, El Kareh B, Balster S, Steinmann P and Yasuda H 2007 *IEEE Trans. Nucl Sci.* **54** 2245

[2] Chen T, Sutton A K, Bellini M, Haugerud B M, Comeau J P, Liang Q, Cressler J D, Cai J, Ning T H, Marshall P W and Marshall C J 2005 *IEEE Trans. Nucl. Sci.* **52** 2353

[3] Cressler J D, Krithivasan R, Zhang G, Niu G F, Marshall P W, Kim H S, Reed R A, Palmer M J and Joseph A J 2002 *IEEE Trans. Nucl. Sci.* **49** 3203

[4] Cresler J D 2013 *IEEE Trans. Nucl. Sci.* **60** 1992

[5] Pellish J A and Cohn L M 2013 *Extreme environment electronics*, Eds. Cressler J D and Mantooth H A (Boca Raton, FL: CRC Press) Ch. 6

[6] Davidović D, Ying H, Dark J. Wier B R, Ge L, Lourenco N E, Omprakash A P, Mourigal M and Cressler J D 2017 *Phys. Rev. Appl.* **8** 024015

[7] Marshall P W, Carts M A and Campbell A 2000 *IEEE Trans. Nucl. Sci.* **47** 2669

[8] Ramachandran V, Gadlage M J, Ahlbin J R, Narasimham B, Alles M L, Reed R A, Bhuva B L, Massengill L W, Black J D and Foster C N 2010 *Solid-State Electronics.* **54** 1052

[9] Huang Y T, C X H, Yang J Q, Ying T, Yu X Q, Dong L, Li W Q and Li X J 2022 *Chin. Phys. B* **31** 028502

[10] Li P 2019 *Enhanced low dose rate sensitivity of silicon-germanium heterojunction bipolar transistor*, Ph. D. dissertation (Xi'an: Xi'an Jiaotong University Press)

[11] Kim H Y, Lo C F, Liu L, Ren F, Kim J and Pearton S J 2022 *Appl. Phys. Lett.* **100** 012107

[12] Laird J S, Hirao T, Onoda S, Mori H and Itoh H 2002 *IEEE Trans. Nucl. Sci.* **49** 1389

[13] Nergui D, Ildefonso A, Tzintzarov G N, Lourenco N E, Omprakash A P, Goley P S, Fleetwood Z E, LaLumondiere S D, Bonsall J P, Monahan D M, Kettering H, Brewe D L and Cressler J D 2020 *IEEE Trans. Nucl. Sci.* **67** 91

[14] Luo J H, Wang Y, Bao M T, Li X J, Yang J Q and Cao F 2022 *IEEE Trans. Dev. Mater. Reliab.* **22** 431

[15] Zhou J C, Wang Y, Li X J, Yang J Q, Bao M T and Cao F 2022 *IEEE Trans. Electron Dev.* **69** 3283

[16] Wei J N, Guo C H, Li P, Li Y H and Guo H X 2019 *Chin. Phys. B* **28** 076106

[17] Varadharajaperumal M, Niu G F, Krithivasan R, Cressler J D, Reed R A, Marshall P W, Vizkelethy G, Dodd P E and Joseph A J 2003 *IEEE Trans. Nucl. Sci.* **50** 2191

[18] Feng Y H, Guo H X, Pan X Y, Zhang J X, Zhong X L, Zhang H, J A A, Liu Y and Ouyang X Y 2022 *Chin. Phys. B* **32** 066105

[19] Sun Y B, Fu J, Wang Y D, Zhou W, Liu Z, Liu X and Shi Y 2016 *Microelectron. Reliab.* **65** 41

[20] Li P, Guo H X, Guo Q, Zhang J X and Wei Y 2015 *Chin. Phys. Lett.* **32** 088505

[21] Niu G F 2010 *J. Electrochem. Soc.* **33** 287

[22] Prakash A P G 2006 *IEEE Trans. Nucl. Sci.* **53** 3175

[23] Cao J, Xu L, Wen S J, Fung R, Narasimham B, Massengill L W and Bhuva B L 2020 *IEEE international reliability physics symposium* (IRPS) p. 15

[24] Sutton A K, Moen K, Cresser J D, Carts M A, Marshall P W, Pellish J A, Ramachandran V, Reed R A, Alles M L and Niu G F 2008 *Solid-State Electron.* **52** 1652

[25] Guo G, Hirao T, Laird J S, Onoda S, Wakasa T, Yamakawa T and Kamiya T 2004 *IEEE Trans. Nucl. Sci.* **51** 2834

[26] Ying H, Wier B R, Dark J, Lourenco N E, Ge L, Omprakash A P, Mourigal M, Davidovic D and Cresler J D 2017 *IEEE Electron Dev. Lett.* **38** 12

[27] Xu Z Y, Niu G F, Luo L, Cressler J D, Alles M L, Reed R, Mantooth H A, Holmes J and Marshall P W 2010 *IEEE Trans. Nucl. Sci.* **57** 3206

[28] Gnana Prakash A P, Hegde V N, Pradeep T M, Pushpa N, Bajpai P K, Patel S P, Trivedi T and Cressler J D 2018 *Radiat. Eff. Defects Solids.* **172** 922

[29] Laird J S, Chen Y, Vo T, Edmonds L, Scheick L and Adell P 2009 *IEEE Trans. Nucl. Sci.* **56** 220

[30] Cressler J D, Comfort J H, Crabbe E F, Patton G L, Stork J M C, Sun J Y C and Meyerson B S 1993 *IEEE Trans. Electron Dev.* **40** 525

[31] Zhang J X, Guo H X, Pan X Y, Guo Q, Zhang F Q, Feng J, Wang X, Wei Y and Wu X X 2018 *Chin. Phys. B* **27** 108501

[32] Chen S Y, Y X, Wu L, Yao S, Li X L, Wang X, Liu M H, Xi S X, Wang L B, Sun J, He C F and Guo Q 2020 *Chin. Phys. Lett.* **37** 046101

[33] Teng J W, Ildefonso A, Tzintzarov G N, Ying H, Moradinia A, Wang P F, Liu X, Zhang E X and Fleetwood D M 2021 *IEEE Trans. Nucl. Sci.* **68** 949

[34] Sun Y B, Liu Z Y, Li X J and Shi Y L 2018 *Radiat. Phys. Chem.* **151** 84